

Parallel or Reversible Reactions? Complications in the Substitution Kinetics of Octahedral Metal Carbonyl Complexes

Karen J. Schneider and Rudi van Eldik*

Institute for Inorganic Chemistry, University of Witten/Herdecke, Stockumer Strasse 10, 5810 Witten, FRG

Received April 19, 1989

The substitution of CO by trimethyl phosphite in Mo(phen)(CO)₄ and Cr(phen)(CO)₄ was studied at temperatures from 25 to 55 °C and ligand concentrations of 6 × 10⁻³ to ~4 M in various solvents under conditions of nitrogen and carbon monoxide saturation. The reverse reaction, viz. the substitution of P(OMe)₃ by CO in M(phen)(CO)₃P(OMe)₃, was also investigated. In the case of molybdenum a two-term rate law with $k_{\text{obs}} = k_i + k_L[\text{phosphite}]$ was confirmed ($k_i = (1.79 \pm 0.02) \times 10^{-4} \text{ s}^{-1}$, $k_L = (1.48 \pm 0.05) \times 10^{-4} \text{ M}^{-1} \text{ s}^{-1}$ at 50 °C in dichloroethane), while for chromium the rate decreased rapidly with increasing phosphite concentration under carbon monoxide saturation, reaching a limiting value of $k_{\text{obs}} = (4.37 \pm 0.07) \times 10^{-4} \text{ s}^{-1}$ in dichloroethane at 50 °C. The rate of the reverse reaction for the latter case under the same conditions is $(2.4 \pm 0.4) \times 10^{-3} \text{ s}^{-1}$. The significance of the reverse reaction is emphasized. The two-term rate law is discussed in terms of parallel associative and dissociative pathways, all involving reversible reactions.

Introduction

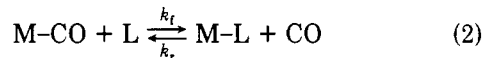
Early studies on coordinatively saturated octahedral metal centers indicated that these reacted via a purely dissociative mechanism.¹ In fact, Tolman summarized the mass of data in a rule which states that organometallic reactions proceed only via intermediates containing 16 or 18 valence electrons.² This precludes an associative mechanism at an 18-electron metal center. Certain apparent exceptions to Tolman's rule were explained by invoking metal to ligand charge transfer (in NO complexes) or ring slippage (cyclopentadienyl, arene, and indenyl complexes) in order to reduce the formal electron count in the intermediate.³ There has been renewed interest in this field recently, and Basolo has extended the scope by studying heterocyclic π -ligands.^{3b} Furthermore, 18-electron cluster carbonyls are exceptionally susceptible to associative attack.⁴ The avoidance of the energetically unfavorable 20-electron configuration has been rationalized by the migration of a metal electron pair to a terminal CO to form a bridging CO. Some examples that cannot be explained in this way involve mononuclear metal carbonyl complexes. These are found to have a two-term rate law, where the second term depends on the incoming ligand concentration.⁵ The interpretation that competitive associative (k_L) and dissociative (k_i) pathways are operating, yielding eq 1, where k_i and k_L are obtained respectively

$$k_{\text{obs}} = k_i + k_L[L] \quad (1)$$

from the intercept and slope of a plot of k_{obs} vs ligand concentration, is still not unequivocal. Furthermore, Huggins et al. recently reported the enhancement both of k_i and k_L , on replacing the cyclopentadienyl ligand with an indenyl ligand.⁶ They pointed out that this effect

cannot be accounted for by ring slippage of the indenyl ligand, but no satisfactory explanation could be offered.

In our studies on such two-term rate law systems, we have noticed that a common complicating factor (even with strong nucleophiles such as P(C₄H₉)₃) appears to be a significant reverse reaction as shown in (2), where M represents the moiety that remains intact during substitution and L is a nucleophile bonding through N or P.



Some of these reverse reactions have been studied in detail elsewhere.⁷ However, none of the mechanisms attempting to account for the observed two-term rate law have thus far considered the possibility of a reverse reaction that can partially or completely account for the k_i term in (1).

As we wished to study the high pressure dependence of k_i and k_L in order to clarify the intimate mechanism, we required a system where both rates were appreciable at 60 °C or below. We thus chose to reinvestigate the substitution reactions of Mo(phen)(CO)₄ and Cr(phen)(CO)₄ (phen = 1,10-phenanthroline) with L = P(OMe)₃, during which the tricarbonyl phosphito complex is formed under conditions of static CO or N₂ saturation (i.e. in a closed system previously saturated with gas). Here we report our findings at ambient pressure.

Experimental Section

General Procedures and Instrumentation. All solutions were prepared with use of dried and distilled solvents, saturated with nitrogen or carbon monoxide by bubbling the required gas through the solvent for at least 15 min. UV-visible spectra and kinetics were measured on a Shimadzu UV-250 or a Hitachi U-3200 spectrophotometer, each fitted with a cell programmer electronically thermostated to within 0.1 °C.

Trimethyl phosphite (Merck) was distilled under vacuum (40 mmHg) and stored for up to 10 days in the dark at -4 °C under the required gas. Mo(phen)(CO)₄ and Cr(phen)(CO)₄ were prepared from Mo(CO)₆ (Riedel-de-Haen) or Cr(CO)₆ (Ventron) and 1,10-phenanthroline hydrate (Sigma) by literature methods⁸ and

(1) (a) Basolo, F.; Pearson, R. G. *Mechanisms of Inorganic Reactions*, 2nd ed.; Wiley: New York, 1967; Chapter 3. (b) Werner, H. *J. Organomet. Chem.* **1966**, *5*, 100. (c) Werner, H.; Prinz, R. *Chem. Ber.* **1966**, *99*, 3582. (d) Angelici, R. J.; Graham, J. R. *J. Am. Chem. Soc.* **1965**, *87*, 5586.

(e) McKerley, B.; Faber, G. C.; Dobson, G. R. *Inorg. Chem.* **1975**, *14*, 2275.

(2) Tolman, C. A. *Chem. Soc. Rev.* **1972**, *1*, 337.

(3) (a) Basolo, F. *Inorg. Chim. Acta* **1985**, *100*, 33. (b) Basolo, F. *Pure Appl. Chem.* **1988**, *60*, 1193.

(4) Poe, A. J. *Pure Appl. Chem.* **1988**, *60*, 1209.

(5) (a) Graham, J. R.; Angelici, R. J. *J. Am. Chem. Soc.* **1966**, *88*, 3658.

(b) Graham, J. R.; Angelici, R. J. *Inorg. Chem.* **1967**, *6*, 2082. (c) Al-Kathumi, K. M.; Kane-Maguire, L. A. P. *J. Inorg. Nucl. Chem.* **1972**, *3759*. (d) Dobson, G. R.; Rettenmaier, A. J. *Inorg. Chim. Acta* **1972**, *6*, 507. (e) Covey, W. D.; Brown, T. L. *Inorg. Chem.* **1973**, *12*, 2820. (f) Pardue, J. E.; Memering, M. M.; Dobson, G. R. *J. Organomet. Chem.* **1974**, *71*, 407. (g) Pardue, J. E.; Dobson, G. R. *Inorg. Chim. Acta* **1976**, *20*, 207. (h) Howell, J. A. S.; Burkinshaw, P. M. *Chem. Rev.* **1983**, *83*, 557. (i) Dobson, G. R.; Binzet, N. Z. *J. Coord. Chem.* **1984**, *13*, 153.

(6) Turaki, N. N.; Huggins, J. M.; Lebiada, L. *Inorg. Chem.* **1988**, *27*, 424.

(7) (a) Hyde, C. L.; Darensbourg, D. J. *Inorg. Chem.* **1973**, *12*, 1286. (b) Darensbourg, D. J. *Adv. Organomet. Chem.* **1982**, *21*, 113. (c) Dobson, G. R.; Smith, L. H. *Inorg. Chem.* **1970**, *9*, 1001.

(8) (a) Bock, H.; tom Dieck, H. *Angew. Chem.* **1966**, *78*, 549. (b) Bock, H.; tom Dieck, H. *Chem. Ber.* **1967**, *100*, 228. (c) Brunner, H.; Herrmann, W. A. *Chem. Ber.* **1972**, *105*, 770. (d) Manuta, D. M.; Lees, A. J. *Inorg. Chem.* **1983**, *22*, 572. (e) Schadt, M. J.; Lees, A. J. *Inorg. Chem.* **1986**, *25*, 672. (f) Wieland, S. Doctoral Thesis, University of Frankfurt, 1988.

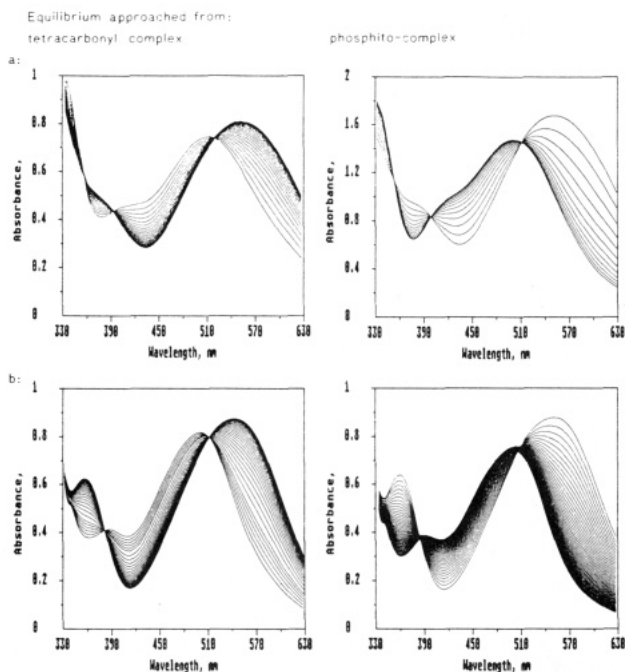


Figure 1. Spectral changes for the forward and reverse reactions of (a) chromium in $(\text{DCE})_{\text{CO}}$ and (b) molybdenum in $(\text{toluene})_{\text{CO}}$ for the following reaction at 50°C : $\text{M}(\text{phen})(\text{CO})_4 + \text{P}(\text{OMe})_3 \rightleftharpoons \text{M}(\text{phen})(\text{CO})_3(\text{P}(\text{OMe})_3) + \text{CO}$.

recrystallized from benzene. $\text{Mo}(\text{phen})(\text{CO})_3(\text{P}(\text{OMe})_3)$ and $\text{Cr}(\text{phen})(\text{CO})_3(\text{P}(\text{OMe})_3)$ were prepared from $\text{M}(\text{phen})(\text{CO})_4$ and trimethyl phosphite according to the method of Houk and Dobson.⁹ All analyses and spectral data were satisfactory.¹⁰

Kinetics. A 10-cm^3 solution of the required complex concentration $((1.0\text{--}1.4) \times 10^{-4}\text{ M})$ and ligand concentration in N_2 - or CO -saturated toluene or dichloroethane (DCE) was prepared under the required gas, with use of gastight Hamilton syringes and septum techniques. Glass cuvettes were evacuated and then filled with solution and sealed with an airtight stopper under a constant stream of gas. The solutions were thermostated, and the disappearance (or appearance in the case of the reverse reaction with no added ligand) of the d-d band at 400 nm for Mo and 430 nm for Cr was monitored continuously after the required temperature had been reached. Reactions were followed for $2^{1/2}$ half-lives, and values of k_{obs} were obtained by using the method of Swinbourne.¹¹ In general the rate constants are an average of three repetitions, which are reproducible to within 5%. As a control, kinetics on a solution of $\text{Mo}(\text{phen})(\text{CO})_4$ under CO and with $0.5\text{ M P}(\text{OMe})_3$ were followed at 360 and 400 nm (maxima of complex) and 540 nm (CT maximum of product), until the infinity values were reached. Values of k_{obs} , obtained from plots of $\ln(A - A_\infty)$ against time, were in good agreement with those calculated by the method of Swinbourne at 400 nm . At low ligand concentrations and N_2 -saturation conditions, however, the infinity values, especially at 360 and 540 nm , were adversely affected by decomposition of the complex (see Results).

Results

The observed rate constants at various L concentrations for the reaction (2) are recorded in Table I. The solvents used for $\text{M} = \text{Mo}$ are toluene and dichloroethane (DCE) under N_2 - and CO -saturated conditions. Only the rate

Table I. Observed Rate Constants for the Reaction $\text{M}(\text{phen})(\text{CO})_4 + \text{L} \rightleftharpoons \text{M}(\text{phen})(\text{CO})_3\text{L} + \text{CO}$ ($\text{M} = \text{Mo, Cr}$; $\text{L} = \text{P}(\text{OMe})_3$)

M	solvent	temp, $^\circ\text{C}$	ligand, concn, M	$10^5 k_{\text{obs}}$, s^{-1}		
Mo	$(\text{toluene})_{\text{CO}}$	50.0	0.0	5.2^a		
			0.0497	4.0 ± 0.2		
			0.0994	4.8 ± 0.1		
			0.1491	5.8 ± 0.1		
			0.1989	6.3 ± 0.2		
			0.2983	8.2 ± 0.2		
			0.3977	10.0 ± 0.3		
			4.00	77 ± 2^b		
			$(\text{toluene})_{\text{N}_2}$	35.0	0.0973	0.69 ± 0.03
					0.3004	1.58 ± 0.01
					0.4998	2.46 ± 0.01
					0.0973	1.47 ± 0.04
	0.3004	2.91 ± 0.06				
	0.4998	4.4 ± 0.2				
	40.1	45.5	0.0994	2.7 ± 0.1		
			0.2983	5.0 ± 0.1		
			0.4997	7.5 ± 0.1		
			0.0994	5.35 ± 0.06		
			0.1989	7.9 ± 0.7		
			0.2983	9.06 ± 0.07		
	$(\text{DCE})_{\text{CO}}$	50.0	0.3977	10.1 ± 0.2		
			0.4998	12.3 ± 0.2		
			0.0994	9.2 ± 0.9		
			0.2983	13.2 ± 0.1		
0.4997			19.0 ± 0.6			
0.0973			1.30 ± 0.02			
0.3131			1.71 ± 0.03			
0.6021			2.39 ± 0.03			
0.0973			4.87 ± 0.03			
0.3131			5.97 ± 0.03			
0.6021			7.56 ± 0.01			
$(\text{DCE})_{\text{N}_2}$			50.0	0.0973	9.8 ± 0.7	
	0.3131	11.72 ± 0.09				
	0.6021	14.75 ± 0.04				
	0.0998	19.3 ± 0.3				
	0.2962	22.1 ± 0.6				
	0.4020	23 ± 1				
	0.5924	26.7 ± 0.7				
	4.231	85 ± 4^c				
	0.0973	32.8 ± 0.3				
	0.3131	40.8 ± 0.3				
	0.6021	47 ± 3				
	$(\text{DCE})_{\text{N}_2}$	50.0		0.0508	19.2 ± 0.1	
0.2031			21.4 ± 0.1			
0.3977			24.4 ± 0.3			
0.6008			26.8 ± 0.3			
0.3			12.7 ± 0.5			
0			240 ± 40^a			
Cr	$(\text{toluene})_{\text{CO}}$	50.0	2.5×10^{-3}	190 ± 10^a		
			6.1×10^{-3}	120 ± 9^a		
			6.1×10^{-3}	116 ± 9		
			8.45×10^{-3}	112 ± 4		
			0.0169	78 ± 8		
			0.051	56 ± 3		
	$(\text{DCE})_{\text{CO}}$	50.0	0.0762	53 ± 4		
			0.1003	51 ± 1		
			0.203	48 ± 2		
			0.398	45.7 ± 0.5		
			0.601	43.6 ± 0.7		
			0.804	43.7 ± 0.5		

^a From reverse reaction. ^b Calculated from extrapolation of low-concentration data: 72 s^{-1} . ^c Calculated by extrapolation: 81 s^{-1} .

constants for CO -saturated DCE are quoted for $\text{M} = \text{Cr}$.

Clear evidence for a reverse reaction was obtained from the final absorbances of solutions with identical complex concentrations ($1.55 \times 10^{-4}\text{ M}$) but with 0.1 and $0.5\text{ M P}(\text{OMe})_3$, even when the kinetics were performed under static conditions of N_2 saturation. Thus, the buildup of CO in solution is sufficient to establish an equilibrium situation. Both $\text{Mo}(\text{phen})(\text{CO})_3(\text{P}(\text{OMe})_3)$ and $\text{Cr}(\text{phen})(\text{CO})_3(\text{P}(\text{OMe})_3)$ were shown to react with CO to

(9) (a) Houk, L. W.; Dobson, G. R. *Inorg. Chem.* **1966**, *5*, 2119. (b) Houk, L. W.; Dobson, G. R. *J. Chem. Soc. A* **1966**, 317.

(10) Analyses were performed at the Microanalytisches Labor Beller, Göttingen, FRG. Anal. Found (calcd) for $\text{Cr}(\text{phen})(\text{CO})_4$: C, 55.76 (55.82); H, 2.55 (2.35); N, 8.14 (8.14). Found (calcd) for $\text{Cr}(\text{phen})(\text{CO})_3(\text{P}(\text{OMe})_3)$: C, 50.09 (49.09); H, 4.4 (3.9); N, 6.41 (6.36); P, 7.67 (7.03). Found (calcd) for $\text{Mo}(\text{phen})(\text{CO})_4$: C, 49.15 (49.48); H, 2.17 (2.06); N, 7.10 (7.22). Found (calcd) for $\text{Mo}(\text{phen})(\text{CO})_3(\text{P}(\text{OMe})_3)$: C, 45.08 (44.64); H, 3.81 (3.54); N, 5.75 (5.78); P, 6.55 (6.39).

(11) Swinbourne, E. S. *J. Chem. Soc.* **1960**, 2371.

Table II. Rate Constants at 50 °C and Corresponding Activation Parameters for the Reaction $M(\text{phen})(\text{CO})_4 + L = M(\text{phen})(\text{CO})_3L + \text{CO}$ ($M = \text{Mo}, \text{Cr}; L = \text{P}(\text{OMe})_3$)^a

M = Mo						
solvent	$10^4 k_f, \text{s}^{-1}$	$10^4 k_L, \text{M}^{-1} \text{s}^{-1}$	$\Delta H_f^\ddagger, \text{kJ mol}^{-1}$	$\Delta S_f^\ddagger, \text{J K}^{-1} \text{mol}^{-1}$	$\Delta H_L^\ddagger, \text{kJ mol}^{-1}$	$\Delta S_L^\ddagger, \text{J K}^{-1} \text{mol}^{-1}$
(DCE) _{CO}	1.79 ± 0.02	1.48 ± 0.05	111 ± 2	27 ± 6	81 ± 4	-67 ± 11
(DCE) _{N₂}	1.86 ± 0.02	1.41 ± 0.04				
(toluene) _{CO}	0.31 ± 0.01	1.72 ± 0.05				
(toluene) _{N₂}	0.41 ± 0.05	1.6 ± 0.2	135 ± 9	85 ± 30	69 ± 2	-106 ± 6
M = Co						
solvent	$10^4 k_1, \text{s}^{-1}$	$10^4 k_{-2}, \text{s}^{-1}$	$\Delta H_1^\ddagger, \text{kJ mol}^{-1}$	$\Delta S_1^\ddagger, \text{J K}^{-1} \text{mol}^{-1}$	$\Delta H_{-2}^\ddagger, \text{kJ mol}^{-1}$	$\Delta S_{-2}^\ddagger, \text{J K}^{-1} \text{mol}^{-1}$
(DCE) _{CO}	4.37 ± 0.07	24 ± 4 ^b	123 ± 1	71 ± 3	117 ± 2	65 ± 7

^a For definitions of k_f , k_L , k_1 , and k_2 , see text. ^b From reverse reaction.

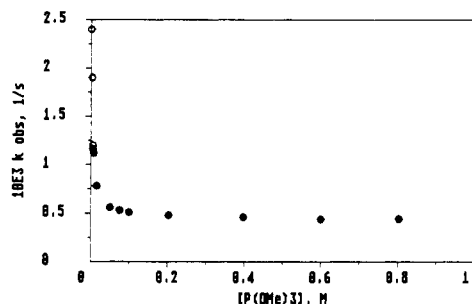
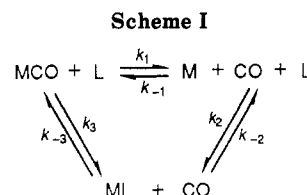


Figure 2. Plot of k_{obs} vs $[\text{P}(\text{OMe})_3]$ for the reaction $\text{Cr}(\text{phen})(\text{CO})_4 + \text{P}(\text{OMe})_3 = \text{Cr}(\text{phen})(\text{CO})_3\text{P}(\text{OMe})_3 + \text{CO}$ at 50 °C in (DCE)_{CO}: (O) data from forward reaction; (*) data from reverse reaction.

form $M(\text{phen})(\text{CO})_4$ when dissolved in CO-saturated solvents. Figure 1 shows the spectral changes for the forward reaction with 0.5 M phosphite concentration, and the reverse reaction with no added phosphite, of chromium in CO-saturated DCE (a) and of molybdenum in CO-saturated toluene (b). In the latter, the isosbestic point at 515 nm is maintained for 2 half-lives but is lost thereafter due to decomposition of $\text{Mo}(\text{phen})(\text{CO})_4$ in the absence of a capturing ligand. An attempt to obviate this problem by following the reverse reaction under low phosphite concentration revealed that, in the case of molybdenum, the equilibrium lies far to the product side and the absorbance change was too small to follow accurately. Also included in Table I are the rate constants for the reverse reaction, k_r , of reaction 2, at a few very low phosphite concentrations.

Angelici and Graham^{12a} reported a lack of dependence on ligand concentration for the substitution of CO by $\text{P}(\text{OMe})_3$ in $\text{Cr}(\text{phen})(\text{CO})_4$ under nitrogen-saturated conditions. In our work we noticed that very curved $\ln k_{\text{obs}}$ vs time plots were obtained under these conditions, especially at higher concentrations of complex and at low ligand concentrations. Under CO saturation, excellent linear plots were obtained. The rate decreased very rapidly with increasing phosphite concentration, reaching a limiting value at $k_{\text{obs}} = (4.37 \pm 0.07) \times 10^{-4} \text{ s}^{-1}$ (see Figure 2). Points obtained from the forward reaction (Figure 2, O) at very low ligand concentrations are in excellent agreement with those obtained from the reverse reaction (Figure 2, *).

The substitution of CO by $\text{P}(\text{OMe})_3$ in $\text{Mo}(\text{phen})(\text{CO})_4$ in DCE and toluene obeys a two-term rate law, as reported by Angelici and Graham,¹² even under carbon monoxide saturation. The plot of k_{obs} vs $[\text{P}(\text{OMe})_3]$ up to a concentration of 0.6 M is linear, and the rate constant in both toluene and DCE at a phosphite concentration of 4 M is in remarkable agreement with the value calculated from



the extrapolated line (see Table I). Table II summarizes the rate constant data and the corresponding activation parameters. The results under N_2 and CO saturation for $M = \text{Mo}$ are very similar. The intercepts are minimally larger and the slopes minimally smaller under N_2 than under CO. The decomposition of $\text{Mo}(\text{phen})(\text{CO})_4$ under N_2 -saturated conditions mentioned above would result in too high a value for the rate constants at low ligand concentrations. Such decomposition, the rate of which decreases in the presence of L and does not interfere with the substitution kinetics, has also been reported by Macholdt and Elias¹³ on other molybdenum pentacarbonyl and tetracarbonyl systems.

Discussion

In Scheme I we consider a situation where the overall forward reaction is a competitive associative and dissociative process and each step is reversible. Under high enough concentrations of L and CO, to ensure pseudo-first-order conditions for all elementary steps, the observed rate constant (with the steady-state approximation applying to M) will have the form given in (3).

$$k_{\text{obs}} = \frac{k_1 k_2 [\text{L}] + k_{-1} k_{-2} [\text{CO}]}{k_{-1} [\text{CO}] + k_2 [\text{L}]} + k_{-3} [\text{CO}] + k_3 [\text{L}] \quad (3)$$

When the kinetic work is performed with constant passage of inert gas through the solution, allowing no buildup of carbon monoxide, $[\text{CO}] = 0$ and eq 3 simplifies to (4), which is identical with the familiar equation (1).

In the absence of the dissociative path, but under saturation with CO, eq 3 is modified to (5), which has the same form as (4), and a plot of $(k_{\text{obs}})_{\text{CO}}$ vs $[\text{L}]$ will result in a slope of k_3 and an intercept of $k_{-3} [\text{CO}]$, which now represents the contribution of the reverse step instead of the dissociative process as in (4). It is important to note

$$(k_{\text{obs}})_{\text{Ar}} = k_1 + k_3 [\text{L}] \quad (4)$$

$$(k_{\text{obs}})_{\text{CO}} = k_{-3} [\text{CO}] + k_3 [\text{L}] \quad (5)$$

that the presence of an intercept under conditions of CO saturation does not necessarily indicate a competing dissociative pathway. The importance of the first term of eq 3 depends on the relative magnitudes of k_1 , k_2 , k_{-1} , k_{-2} , $[\text{CO}]$, and $[\text{L}]$. Furthermore, regardless of the occurrence

(12) (a) Angelici, R. J.; Graham, J. R. *Inorg. Chem.* 1967, 6, 988. (b) Angelici, R. J.; Graham, J. R. *Inorg. Chem.* 1967, 6, 992.

(13) Macholdt, H.-T.; Elias, H. *Inorg. Chem.* 1984, 23, 4315.

of a dissociative path or not, under conditions of CO saturation the observed rate constant could be higher than under a stream of inert gas by a contribution of at least $k_{-3}[\text{CO}]$. Such an effect has been reported without satisfactory explanation by Huggins.⁶

We can interpret our results in terms of Scheme I.

Molybdenum. The associative k_3 pathway is important in the Mo system as evidenced in the linearity of the k_{obs} vs $[\text{P}(\text{OMe})_3]$ data, irrespective of the saturation gas. The similarity under both gases suggests that the contribution of the k_1 pathway is also not negligible. We postulate that $k_{-1}[\text{CO}] \ll k_2[\text{L}]$, even at the lowest phosphite concentrations. This is not unreasonable, as the concentration of CO in all our solvents is very low (7.4×10^{-3} M in toluene and 6.0×10^{-3} M in DCE at 25 °C¹⁴) and CO and $\text{P}(\text{OMe})_3$ are not expected to differ substantially in their ability to capture the pentacoordinate intermediate. Furthermore, as the equilibrium lies far to the product side, the approximation $k_1 k_2 [\text{L}] \gg k_{-1} k_{-2} [\text{CO}]$ may be made. Thus, the rate constant expression reduces to (6).

$$(k_{\text{obs}})_{\text{CO}} = k_1 + k_{-3}[\text{CO}] + k_3[\text{L}] \quad (6)$$

The value of the rate constant for the reverse reaction ($[\text{L}] = 0$) in toluene is $5.2 \times 10^{-5} \text{ s}^{-1}$. This represents $k_{-2} + k_{-3}[\text{CO}]$ and compares favorably with the value for $k_1 + k_{-3}[\text{CO}]$ ($3.1 \times 10^{-5} \text{ s}^{-1}$) obtained from the intercept of the k_{obs} vs $[\text{L}]$ plot, where different limiting conditions are valid. The difference represents the difference in rate of dissociation of $\text{X} = \text{CO}$ or $\text{P}(\text{OMe})_3$ from $\text{Mo}(\text{phen})(\text{CO})_3\text{X}$. The relative rates are plausible, as it is to be expected that the dissociation of the large phosphite ligand, which has less back-bonding capability than CO, will be of the same order, though somewhat faster, than the dissociation of CO.

The activation entropies for the ligand-independent and ligand-dependent pathways are positive and negative, respectively, as is expected for D- and A-activated mechanisms. The enthalpy of activation of the k_i route is significantly larger than that of the k_L route, and this difference is more marked in the case of the solvent toluene. The rate for the associative reaction is comparable in DCE and toluene, and the difference in overall rates is accounted for by a slower dissociative reaction in toluene. This fact is clearly a result of the higher enthalpy barrier for the k_1 pathway. This trend in k_i for toluene and DCE parallels the trend in decomposition rates in these solvents.

The kinetic results do not enable us to make a definitive statement about the transition state of each pathway. However, additional information points to the dissociation of CO as the first step in the k_i route. In the absence of a capturing ligand, the complex decomposes via initial reversible loss of CO, indicating the availability of the proposed k_1/k_{-1} pathway. The ligand-dependent route could be ascribed to a phen ring-opening mechanism. The rate of ring closure has been determined by Oishi¹⁵ during the flash-photolytical preparation of $\text{Mo}(\text{phen})(\text{CO})_4$ and is very fast ($k = 5.6 \times 10^3 \text{ s}^{-1}$ at 24 °C). We, however, favor an associative pathway involving significant initial P–Mo bond making for two reasons: first, the phen ligand is not expelled during the reaction as in all other ring-opening systems,¹⁶ and second, an analogous Mo–chelate system, which bonds through sulfur and is more likely to undergo ring opening because of greater chelate flexibility, has been shown to react associatively.¹⁷ Oishi¹⁵ discusses the

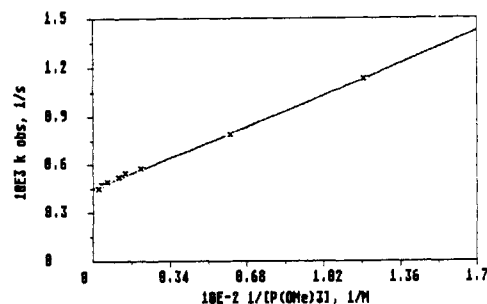


Figure 3. Plot of k_{obs} vs $1/[\text{P}(\text{OMe})_3]$ for the reaction $\text{Cr}(\text{phen})(\text{CO})_4 + \text{P}(\text{OMe})_3 \rightleftharpoons \text{Cr}(\text{phen})(\text{CO})_3(\text{P}(\text{OMe})_3) + \text{CO}$ at 50 °C in $(\text{DCE})_{\text{CO}}$ for phosphite concentrations from 6.1×10^{-3} to 0.8 M.

possibility of considerable interaction between the not yet coordinated nitrogen and the metal in his ring-opened intermediate. It is quite possible that, in our system, the transition state for the associative route involves bond lengthening of one Mo–N and one Mo–C bond.

Chromium. In the absence of an associative path the last two terms of eq 3 fall away and two limiting forms are possible for the rate expression. If $k_{-1}[\text{CO}] \gg k_2[\text{L}]$, eq 7a holds

$$k_{\text{obs}} = k_{-2} + \frac{k_1 k_2}{k_{-1}[\text{CO}]}[\text{L}] \quad (7a)$$

while if $k_2[\text{L}] \gg k_{-1}[\text{CO}]$, the appropriate expression is given by (7b).

$$k_{\text{obs}} = k_1 + \frac{k_{-1} k_{-2} [\text{CO}]}{k_2 [\text{L}]} \quad (7b)$$

A plot of k_{obs} vs $[\text{L}]$ will be curved, approaching a limiting value of k_1 as the second term in (7b) becomes negligibly small. The shape of the curve (convex or concave up) will be determined by the relative magnitudes of k_{-2} and k_1 .¹⁸ The ligand dependence for $\text{Cr}(\text{phen})(\text{CO})_4$ is best described by the limiting conditions $k_2[\text{L}] \gg k_{-1}[\text{CO}]$, as in the case of molybdenum, and hence rate constant expression (7b).

The results show that, in the case of $\text{Cr}(\text{phen})(\text{CO})_4$, k_{-2} is approximately 6 times larger than k_1 and the expected curve (Figure 2) is obtained. As corroboration of an equilibrium situation, the rate is the same irrespective of whether the equilibrium is approached from the left or the right. A plot of k_{obs} vs $1/[\text{L}]$ is linear for $[\text{L}] = 8.45 \times 10^{-3}$ to 0.8 M (Figure 3), as predicted by (7b). The value of k_1 from this plot ($(4.43 \pm 0.05) \times 10^{-4} \text{ s}^{-1}$) is in excellent agreement with the limiting value obtained from high ligand concentrations ($4.4 \times 10^{-4} \text{ s}^{-1}$). With use of the estimated carbon monoxide concentration of 6×10^{-3} M (see above¹⁴) and the experimental value for k_{-2} , the ratio k_{-1}/k_2 obtained from the slope is 0.4. Thus, the greater basicity of $\text{P}(\text{OMe})_3$ over that of CO plays a marginally more important role than size in the competition for the five-coordinate chromium intermediate.

It may thus be concluded from the kinetic data and activation parameters that a distinctly different mechanistic pathway is available to molybdenum, which is not evident for chromium. This may be understood in terms of the size of the metal (the covalent radius for Mo is ca. 0.15 Å larger than that of chromium). Such a mechanistic

(14) Stephen, H., Stephen, T., Eds. *Solubilities of Inorganic and Organic Compounds*; Pergamon Press: London, 1964; Vol. II.

(15) Oishi, S. *Organometallics* 1987, 7, 1237.

(16) For a brief review see: Dobson, G. R.; Faber, G. C. *Inorg. Chim. Acta* 1970, 4, 87.

(17) Awad, H. H.; Dobson, C. B.; Dobson, G. R.; Leipoldt, J. G.; Schneider, K. J.; van Eldik, R.; Wood, H. E. *Inorg. Chem.* 1989, 28, 1654.

(18) (a) Toma, H. E.; Malin, J. M.; Giesbrecht, E. *Inorg. Chem.* 1973, 12, 2084. (b) Malin, J. M.; Toma, H. E.; Giesbrecht, E. *J. Chem. Educ.* 1977, 54, 385. (c) Abu-Gharib, E. A.; Bin Ali, R.; Blandamer, M. J.; Burgess, J. *Transition Met. Chem.* 1987, 12, 371.

changeover has been noticed for these metals for the displacement of flexible chelate rings bonding through S by phosphines and phosphites¹⁷ and for solvent-exchange processes in the first transition series.¹⁹ In both cases the changeover correlates with metal size and was confirmed by trends in the activation volume. High-pressure kinetic studies are underway to throw more light on the intimate mechanism of the phenanthroline system. Furthermore, Scheme I is a possible explanation for the enhancement of the ligand-independent term in the indenyl system of Huggins et al.⁶ CO has, in general, the effect of increasing the rate of substitution as expected when a reverse reaction is present. The replacement of the cyclopentadienyl ligand by an indenyl ligand lowers the activation energy barrier for the forward, as well as the reverse, associative reaction paths.

(19) Merbach, A.; Ducommun, Y. In *Inorganic High Pressure Chemistry: Kinetics and Mechanisms*; van Eldik, R., Ed.; Elsevier: Amsterdam, 1986; Chapter 2.

Conclusions

We have shown that the reverse reaction of $M(\text{phen})(\text{CO})_3\text{L}$ with CO makes the system more complicated than initially thought. Disregard of this possibility is likely to lead to false conclusions.

As shown in eq 5, the presence of a two-term rate law need not necessarily imply competing reactions but can be ascribed to the reverse reaction. The molybdenum system studied in this work appears to react via competing associative and dissociative pathways, but each case must be considered separately. Compounds that are stable in solution could well approach equilibrium via a purely associative mechanism, with eq 5 describing the observed rate constant.

Acknowledgment. We gratefully acknowledge financial support from the Deutsche Forschungsgemeinschaft, the Fonds der Chemischen Industrie, and the Volkswagen-Stiftung.

Reactions of Transition-Metal σ -Acetylide Complexes. 14.¹ Cyclobutenyl, Butadienyl, and Allyl Complexes of Ruthenium Derived from 1,1-Dicyano-2,2-bis(trifluoromethyl)ethene. X-ray Structures of $\text{Ru}[\text{C}=\text{CPhC}(\text{CF}_3)_2\text{C}(\text{CN})_2](\text{CO})(\text{PPh}_3)(\eta\text{-C}_5\text{H}_5)$, $\text{Ru}[\text{C}(\text{CN})_2\text{CX}=\text{C}(\text{CF}_3)_2](\text{CO})(\text{PPh}_3)(\eta\text{-C}_5\text{H}_5)$ ($\text{X} = \text{Me}$, Ph), and $\text{Ru}[\eta^3\text{-C}(\text{CF}_3)_2\text{CPhC}=\text{C}(\text{CN})_2](\text{PPh}_3)(\eta\text{-C}_5\text{H}_5)$

Michael I. Bruce,* Trevor W. Hambley, Michael J. Liddell, Michael R. Snow,
A. Geoffrey Swincer, and Edward R. T. Tiekink

Jordan Laboratories, Department of Physical and Inorganic Chemistry,
University of Adelaide, Adelaide, South Australia 5001, Australia

Received April 24, 1989

Reactions between $\text{Ru}(\text{C}_2\text{Me})(\text{PPh}_3)_2(\eta\text{-C}_5\text{H}_5)$ or $\text{Ru}(\text{C}_2\text{Ph})(\text{L})_2(\eta\text{-C}_5\text{H}_5)$ ($\text{L}_2 = (\text{PPh}_3)_2$, dppe, $(\text{CO})(\text{PPh}_3)$) and $(\text{CF}_3)_2\text{C}=\text{C}(\text{CN})_2$ gave the corresponding σ -cyclobutenyl complexes, of which $\text{Ru}[\text{C}=\text{CPhC}(\text{CF}_3)_2\text{C}(\text{CN})_2](\text{CO})(\text{PPh}_3)(\eta\text{-C}_5\text{H}_5)$ (**1g**) was fully characterized by X-ray crystallography. Thermal isomerization of the dppe and $(\text{CO})(\text{PPh}_3)$ complexes to the σ -buta-1,3-dien-2-yl derivatives occurred; under CO, two isomers of $\text{Ru}[\text{C}(\text{CN})_2\text{CMe}=\text{C}(\text{CF}_3)_2](\text{CO})(\text{PPh}_3)(\eta\text{-C}_5\text{H}_5)$ were formed. The X-ray structures of one of these (**2h**), and the phenyl analogue (**2g**), were determined. The allyls $\text{Ru}[\eta^3\text{-C}(\text{CF}_3)_2\text{CXC}=\text{C}(\text{CN})_2](\text{PPh}_3)(\eta\text{-C}_5\text{H}_5)$ ($\text{X} = \text{Me}$ (**3d**), Ph (**3g**)) were obtained thermally or photochemically; the structure of **3g** was also determined, thus completing the series σ -cyclobutenyl, σ -butadienyl, η^3 -allyl derived from the same metal/ligand combinations. Crystal data for **1g**: orthorhombic, space group $P2_12_12_1$, $a = 10.409$ (2) Å, $b = 16.227$ (3) Å, $c = 20.000$ (3) Å, $Z = 4$; 2851 data were refined to $R = 0.040$, $R_w = 0.041$. Crystal data for **2g**: monoclinic, space group $P2_1/n$, $a = 14.942$ (1) Å, $b = 13.413$ (2) Å, $c = 16.928$ (6) Å, $\beta = 97.02$ (1)°, $Z = 4$; 3659 data were refined to $R = 0.045$, $R_w = 0.059$. Crystal data for **2h**: monoclinic, space group $C2/c$, $a = 22.237$ (4) Å, $b = 18.648$ (5) Å, $c = 17.731$ (3) Å, $\beta = 124.93$ (2)°, $Z = 8$; 3076 data were refined to $R = 0.039$, $R_w = 0.042$. Crystal data for **3g**: monoclinic, space space $P2_1/n$, $a = 13.804$ (3) Å, $b = 17.257$ (2) Å, $c = 13.957$ (3) Å, $\beta = 98.49$ (2)°, $Z = 4$; 2922 data were refined to $R = 0.055$, $R_w = 0.062$.

Introduction

We have recently described reactions between 1,1-dicyano-2,2-bis(trifluoromethyl)ethene, $(\text{NC})_2\text{C}=\text{C}(\text{CF}_3)_2$ (dcfe), and substituted acetylide complexes containing $\text{W}(\text{CO})_3(\eta\text{-C}_5\text{H}_5)$, $\text{Mn}(\text{CO})_3(\text{dppe})$, or $\text{Fe}(\text{CO})_2(\eta\text{-C}_5\text{H}_5)$

groups, to give the σ -cyclobutenyl complexes (**1a-c**, Scheme I).² The reaction between **1a** and $\text{Me}_3\text{NO}\cdot 2\text{H}_2\text{O}$ afforded the hydrolysis product $\text{W}[\text{NH}=\text{C}(\text{OH})\text{C}(\text{CN})-\text{C}(\text{CN})_2\text{CPh}=\text{C}(\text{CF}_3)_2](\text{CO})_2(\eta\text{-C}_5\text{H}_5)$, formed by addition of

(1) Part 13: Bruce, M. I.; Liddell, M. J.; Tiekink, E. R. T. *J. Organomet. Chem.* 1988, 352, 199.

(2) Bruce, M. I.; Liddell, M. J.; Snow, M. R.; Tiekink, E. R. T. *Organometallics* 1988, 7, 343.